Tightly Bound Trions in Transition Metal Dichalcogenide Heterostructures

Matthew Z. Bellus, Frank Ceballos, Hsin-Ying Chiu,* and Hui Zhao*

Department of Physics and Astronomy, The University of Kansas, Lawrence, Kansas 66045, United States

ABSTRACT We report the observation of trions at room temperature in a van der Waals heterostructure composed of $MoSe_2$ and WS_2 monolayers. These trions are formed by excitons excited in the WS_2 layer and electrons transferred from the $MoSe_2$ layer. Recombination of trions results in a peak in the photoluminescence spectra, which is absent in monolayer WS_2 that is not in contact with $MoSe_2$. The trion origin of this peak is further confirmed by the linear dependence of the peak position on excitation intensity. We deduced a zero-density trion binding energy of 62 meV. The trion formation facilitates electrical control of exciton transport in transition metal dichalcogenide heterostructures, which can be utilized in various optoelectronic applications.

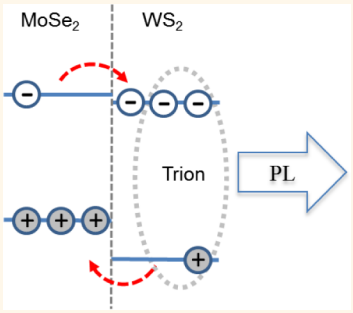

KEYWORDS: transition metal dichalcogenides · van der Waals heterostructure · exciton · trion · charge transfer · photoluminescence

Two-dimensional transition metal dichalcogenides (TMDs) have emerged as a new class of semiconducting nanomaterials. One unique aspect of these materials is the strong Coulomb interaction between electrons and holes due to the lack of dielectric screening of the electric field outside the material. This results in strongly bound excitons with unusually large exciton binding energies on the order of several hundred millielectronvolts (meV),[1,2] and hence provides a unique platform to explore exciton physics and many body interactions. From an application point of view, since these excitons are stable at room temperature, they play dominant roles in determining optical properties of these materials.

Recent studies have revealed that the strong Coulomb interaction in two-dimensional TMDs also leads to formation of tightly bound charged excitons, also known as trions, mostly at cryogenic temperatures. In MoS_2 monolayers, a trion is formed by an exciton with an extra electron or hole, which can be introduced by gate-doping,[3] photoionization of impurities,[4] substrates,[5] or functionalization layers.[6] These trions have been observed in low-temperature photoluminescence (PL),[3−8] electroluminescence,[9] and absorption spectra,[8] as extra peaks on the low-energy side of the neutral exciton peaks. From these measurements, the trion binding energy in MoS_2 was found to be in the range of 18−50 meV,[3−9] which is sensitive to the laser excitation intensity,[4] the doping concentration,[5] and dielectric environment.[7] Moreover, strong sample-to-sample variation of the trion binding energy was also reported.[4] Similarly, trions were also observed in other TMDs by PL,[10−16] electroluminescence,[17] and absorption spectroscopy,[12] including $MoSe_2$ with binding energies of 20−30 meV,[10,11] WS_2 with binding energies of 40−45 meV,[12,13] and WSe_2 with binding energies of 25−30 meV.[14,15] Furthermore, theoretical models on trion states in TMDs have been developed, which are consistent with experimental results.[18,19]

Here we extend studies of trions to van der Waals heterostructures formed by different types of TMD monolayers. Very recently, several types of TMD heterostructures have been fabricated by manual assembly of exfoliated TMD monolayers[20−26] and chemical vapor deposition.[27−30] Since advantages of each participating monolayer can potentially be combined, these heterostructures have shown great promise in applications of field effect transistors,[23,31] vertical tunneling transistors,[32,33] photovoltaic devices,[24,26] and light-emitting devices.[25] We show that efficient charge transfer processes in TMD heterostructures facilitate formation of trions, without external supply of charge carriers. As a model system, we study a heterostructure sample formed by

* Address correspondence to chiu@ku.edu, huizhao@ku.edu.

Received for review April 10, 2015 and accepted June 5, 2015.

Published online June 05, 2015
10.1021/acsnano.5b02144

$MoSe_2$ and WS_2 monolayers. A pronounced trion peak from WS_2 is observed at room temperature in the heterostructure sample, which is absent in WS_2 monolayer. The trion binding energy is found to be about 62 meV, slightly larger than previously reported values in monolayer WS_2,[12,13] and increases linearly with the excitation intensity. The formation of trions facilitates electrical control of exciton transport in TMD heterostructures.

RESULTS AND DISCUSSION

The $MoSe_2$–WS_2 sample is fabricated by a manual transfer technique (see Methods). Flakes of $MoSe_2$ and WS_2 that contain monolayer regions are first exfoliated from bulk crystals to polydimethylsiloxane (PDMS) substrates, as shown in Figure 1a,b, then sequentially transferred to a silicon substrate with a 90 nm SiO_2 layer [Figure 1c,d]. In addition to the heterostructure region, the flake also contains individual monolayers of $MoSe_2$ and WS_2, and hence facilitates direct comparison of the heterostructure and the participating monolayers.

Figure 2 shows the PL spectra measured under the excitation of a continuous-wave 405 nm laser beam, with the laser spot located on the regions of WS_2 monolayer (blue), $MoSe_2$ monolayer (red), and heterostructure (black), respectively. The individual WS_2 and $MoSe_2$ monolayers have PL peaks at about 2.01 and 1.58 eV, respectively, both with widths of about 50 meV. These are consistent with previously reported values,[10,12,13,34–36] and further confirms the monolayer thickness of these flakes. The peak of WS_2 is significantly quenched in the heterostructure, by a factor of about 23. Quenching of PL in heterostructures compared to individual TMD layers has been previously reported,[21,22,27,30] which is caused by charge transfer across the interface: According to first-principles

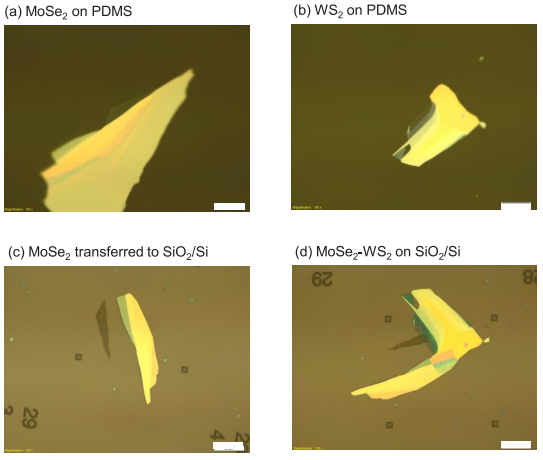

Figure 1. Microscope images of $MoSe_2$ (a) and WS_2 (b) flakes exfoliated on polydimethylsiloxane (PDMS) substrates, the $MoSe_2$ monolayer transferred to SiO_2/Si substrate (c), and the $MoSe_2$–WS_2 heterostructure sample (d) fabricated by transferring the WS_2 flake on top of $MoSe_2$ flake. The scale bars are 20 μm.

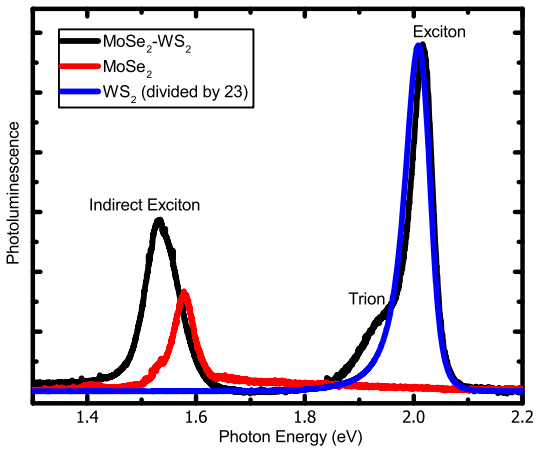

Figure 2. Photoluminescence spectra of the WS_2 monolayer (blue, divided by 23), $MoSe_2$ monolayer (red), and $MoSe_2$–WS_2 heterostructure (black) obtained under the same conditions.

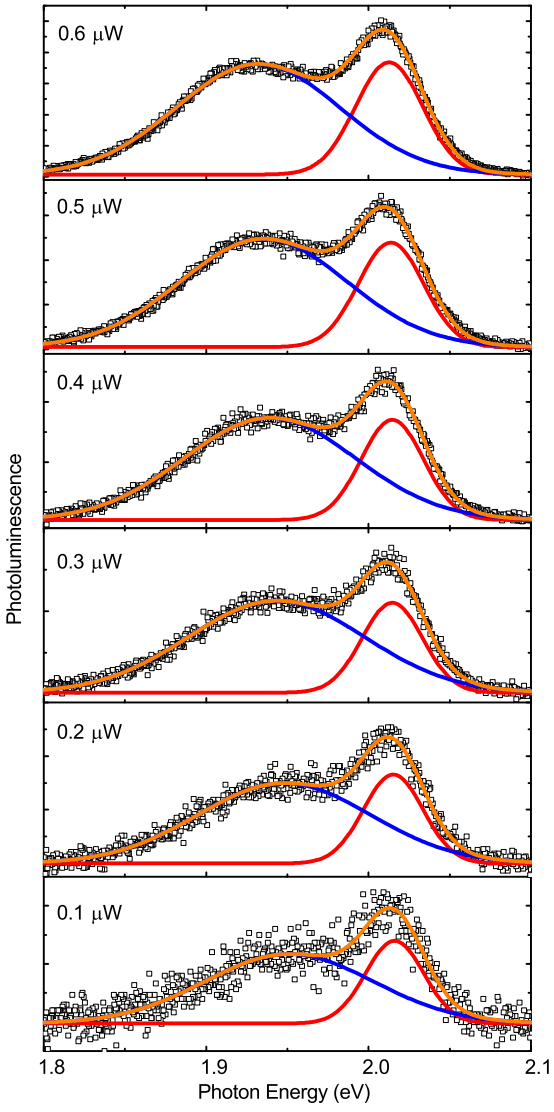

Figure 3. Photoluminescence spectra of $MoSe_2$–WS_2 heterostructure under different excitation powers, as labeled in each panel. The solid orange lines are double-Gaussian-peak fits to the data. The red and blue curves indicate the two peaks.

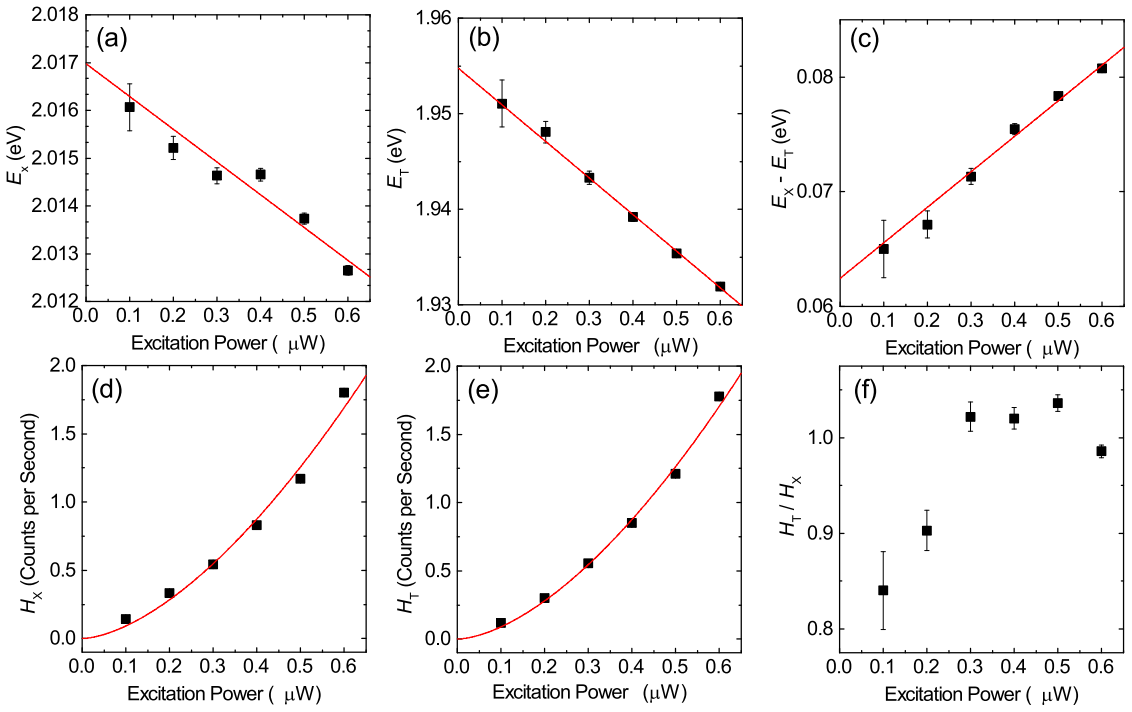

Figure 4. (a–c) The exciton (a) and trion (b) peak positions deduced from the fits shown in Figure 3 and the trion binding energy (c) as a function of the excitation power. The solid lines are linear fits. (d–f) The height of the exciton (d) and trion (e) peaks and the ration between them (f) as a function of the excitation power. The solid lines are power fits.

calculations, most heterostructures formed by two TMD monolayers have type-II band alignments, where the bottom of the conduction band and the top of the valence band are located in different layers.[37−41] Hence, once excited, electrons and holes transfer to different sides of the interface, resulting in formation of spatially indirect excitons, and therefore, the PL peaks of the individual layers are quenched. A strong peak at about 1.53 eV is also observed from the heterostructure. Since it is about 50 meV below the expected $MoSe_2$ exciton peak and about 2 times stronger than the PL from the individual $MoSe_2$ monolayer, we can rule out the excitons in $MoSe_2$ as its origin, and attribute it to indirect excitons formed by electrons in WS_2 and holes in $MoSe_2$. This assignment is also consistent with results of first-principles calculations, which predicted small offsets of conduction bands of 60 meV in $MoSe_2$−WS_2 heterostructures.[38]

A shoulder on the low-energy side of the exciton peak in the heterostructure sample can be clearly seen, which is absent in the spectra of WS_2 monolayer. We assign this feature to trions formed by excitons in WS_2 and electrons transferred from $MoSe_2$. To confirm this assignment, we measure PL spectra of the heterostructure at various excitation powers. The results are shown in Figure 3. We find that this trion peak can be reliably separated from the main exciton peak. By fitting the spectra with two Gaussian functions, shown as the solid lines in Figure 3, we obtain parameters describing the two peaks. These parameters are summarized in Figure 4.

As we increase the excitation level, the energies of the exciton (E_X) and trion peaks (E_T) both decrease, as shown in panels a and b of Figure 4. The change in E_T is about 20 meV in this range, larger than the change of E_X of less than 4 meV. Figure 4c shows that the difference between these two peaks, $E_X - E_T$, increases linearly with the excitation level. This energy difference, known as trion binding energy, is the energy required to convert the trion to an exciton and a free charge (electron or hole). Since the free charge needs to be released to above the Fermi surface where unoccupied states are available, the trion binding energy increases with the Fermi surface, which increases with the excitation level. Previously, the increase of the trion binding energy with carrier density has been observed in monolayer TMDs, such as MoS_2,[3] WS_2,[4] WSe_2,[14] and has been regarded as one of the signatures of trions. From a linear extrapolation, shown as the solid line in Figure 4c, we find a trion binding energy of about 62 ± 2 meV at zero excitation power. This value is similar to, and slightly larger than, the trion binding energies in monolayer WS_2 (40−45 meV) previously reported,[12,13] considering potential sample-to-sample variations of the binding energy.[4]

From the double-peak fits shown in Figure 3, we also deduce the height of the two peaks, H_X and H_T, as a function of the excitation power. The results are summarized in Figure 4d,e. Both peaks increase with the excitation power at a rate faster than linear. By fitting the data, as shown as the solid curves, we find that this increase is of power 1.6 in both cases.

The superlinear increase of PL with excitation power is usually attributed to the presence of defects allowing for nonradiative recombination and trapping of excitons that compete with radiative recombination.[42−44] As the excitation power increases, higher carrier densities are injected, and the fraction of injected carriers that are affected by these defects decreases, resulting in a superlinear increase of PL. Given the very low excitation power used in this study, this mechanism is likely the origin of the observed power dependence. The ratio of the two peaks is relatively constant in the range of the measurement, as shown in Figure 4f.

Previously, trions have been observed in monolayer TMDs when the sample is doped or when extra carriers are introduced by other means. We show that TMD heterostructures allow observation of trions at room temperature without an external source of carriers. We attribute this observation to the efficient charge transfer process in such heterostructures. First-principle calculations[38] have predicted that TMD heterostructures form type-II band alignment with the bottom of the conduction band and the top of the valence band located in different layers. For the heterostructure of $MoSe_2$−WS_2, the predicted band alignment is shown in Figure 5a, with the offsets of 60 and 270 meV in conduction (C) and valence (V) bands, respectively.[38] In this scheme, the exciton binding energy is not included for clarity. The 405 nm pump excites both layers by populating the conduction and valence bands with electrons (−) and holes (+), as shown in Figure 5a. The electrons (holes) injected in $MoSe_2$ (WS_2) are expected to transfer to the lower energy state in WS_2 ($MoSe_2$), indicated by the red dashed line in Figure 5b. Recent time-resolved studies on similar TMD heterostructures, such as MoS_2−WS_2[45] and MoS_2−$MoSe_2$,[46] have shown that the charge transfer across the van der Waals interface is highly efficient and ultrafast. Under the continuous excitation of the 405 nm laser, the interlayer charge transfer process results in extra electrons (holes) in WS_2 ($MoSe_2$) layer. As a consequence, trions are formed in

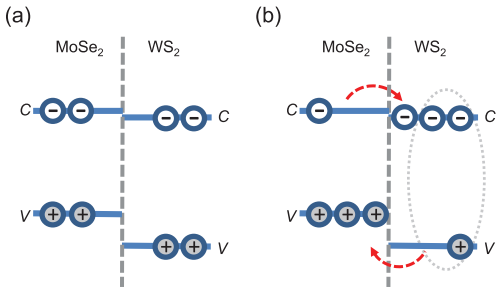

Figure 5. Charge transfer of trion formation in TMD heterostructure. (a) Both layers of the heterostructure are excited by the 405 nm laser beam, with electrons (−) and holes (+) populating the conduction (C) and valence (V) bands. (b) Transfer of electrons and holes across the interface (red dashed lines) results in extra electrons in WS_2, which facilitates trion formation (the gray oval).

WS_2 each with two electrons and one hole, as indicated by the gray dotted shape in Figure 5. We note that Figure 5 also suggests the possibility of formation of positively charged trions in the $MoSe_2$ layer. However, due to the relatively low PL yield of $MoSe_2$, no features related to $MoSe_2$ exctions or trions are observable in the heterostructure sample.

CONCLUSION

In summary, we provide evidence of trion formation in TMD heterostructures at room temperature without external supply of charge carriers. This process is facilitated by, and provides evidence for, ultrafast and efficient charge transfer in TMD heterostructures owing to their type-II band alignment. We found a zero-density trion binding energy of about 62 meV in the $MoSe_2$−WS_2 heterostructure studied. Since most TMD heterostructures are expected to form type-II band alignments, trion formation can be expected in other similar structures as well. Observation of trions in TMD heterostructures opens up a new platform to study excitonic physics in low-dimensional systems and the Coulomb interaction between charge carriers, and can be utilized in optoelectronic devices for electric control of optical excitations.

METHODS

The samples used in this study are fabricated by mechanical exfoliation followed by a manual transfer technique. First, polydimethylsiloxane (PDMS) substrates are made onto glass slides to allow for a rigid and transparent backing. Next, $MoSe_2$ flakes are mechanically exfoliated onto a PDMS substrate. Utilizing an optical microscope, monolayer flakes are easily identified by optical contrast, as shown in Figure 1a. The PDMS substrate with $MoSe_2$ flakes is inverted under the microscope and lowered onto a silicon substrate with a 90 nm oxide layer. Slowly lifting the PDMS substrate allows the $MoSe_2$ monolayer flake to adhere to the silicon substrate, as shown in Figure 1c. The sample is then cleaned in acetone, rinsed with isopropyl alcohol, and dried under nitrogen. To ensure little to no residue from the exfoliation or transfer processes remains, the sample is thermally annealed for 2 h at 200 °C in a H_2/Ar (10 sccm/100 sccm) environment with a pressure of 3 Torr. Next, a WS_2 flake is mechanically exfoliated and processed in the same way, and is precisely transferred on top of the $MoSe_2$ flake. The heterostructure, shown in Figure 1d, is cleaned in acetone and isopropyl alcohol, and thermally annealed to allow for proper contact between the two flakes.

The PL system is based on a Horiba iHR550 imaging spectrometer equipped with a thermoelectrically cooled charge-coupled device (CCD) camera. A diode laser of 405 nm is used for excitation. The laser beam is focused to the sample through a microscope objective lens, to a spot size of less than 1 μm. The PL from the sample is collected by the same objective lens and is guided to the spectrometer. All the measurements are performed with the sample in ambient condition.

Conflict of Interest: The authors declare no competing financial interest.

Acknowledgment. This material is based upon work supported by the National Science Foundation of USA under Award Nos. DMR-0954486 and IIA-1430493.

REFERENCES AND NOTES

1. Chernikov, A.; Berkelbach, T. C.; Hill, H. M.; Rigosi, A.; Li, Y. L.; Aslan, O. B.; Reichman, D. R.; Hybertsen, M. S.; Heinz, T. F. Exciton Binding Energy and Nonhydrogenic Rydberg Series in Monolayer WS_2. *Phys. Rev. Lett.* **2014**, *113*, 076802.
2. He, K.; Kumar, N.; Zhao, L.; Wang, Z.; Mak, K. F.; Zhao, H.; Shan, J. Tightly Bound Excitons in Monolayer WSe_2. *Phys. Rev. Lett.* **2014**, *113*, 026803.
3. Mak, K. F.; He, K.; Lee, C.; Lee, G. H.; Hone, J.; Heinz, T. F.; Shan, J. Tightly Bound Trion in Monolayer MoS_2. *Nat. Mater.* **2013**, *12*, 207–211.
4. Mitioglu, A. A.; Plochocka, P.; Jadczak, J. N.; Escoffier, W.; Rikken, G.; Kulyuk, L.; Maude, D. K. Optical Manipulation of the Exciton Charge State in Single-Layer Tungsten Disulfide. *Phys. Rev. B* **2013**, *88*, 245403.
5. Li, Y.; Qi, Z.; Liu, M.; Wang, Y.; Cheng, X.; Zhang, G.; Sheng, L. Photoluminescence of Monolayer MoS_2 on $LaAlO_3$ and $SrTiO_3$ Substrates. *Nanoscale* **2014**, *6*, 15248–15254.
6. Lin, J. D.; Han, C.; Wang, F.; Wang, R.; Xiang, D.; Qin, S.; Zhang, X. A.; Wang, L.; Zhang, H.; Wee, A. T.; et al. Electron-Doping-Enhanced Trion Formation in Monolayer Molybdenum Disulfide Functionalized with Cesium Carbonate. *ACS Nano* **2014**, *8*, 5323–5329.
7. Lin, Y.; Ling, X.; Yu, L.; Huang, S.; Hsu, A. L.; Lee, Y. H.; Kong, J.; Dresselhaus, M. S.; Palacios, T. Dielectric Screening of Excitons and Trions in Single-Layer MoS_2. *Nano Lett.* **2014**, *14*, 5569–5576.
8. Zhang, C.; Wang, H.; Chan, W.; Manolatou, C.; Rana, F. Absorption of Light by Excitons and Trions in Monolayers of Metal Dichalcogenide: Experiments and Theory. *Phys. Rev. B* **2014**, *89*, 205436.
9. Lopez-Sanchez, O.; Llado, E. A.; Koman, V.; Morral, A. F. I.; Radenovic, A.; Kis, A. Light Generation and Harvesting in a van der Waals Heterostructure. *ACS Nano* **2014**, *8*, 3042–3048.
10. Ross, J. S.; Wu, S.; Yu, H.; Ghimire, N. J.; Jones, A. M.; Aivazian, G.; Yan, J.; Mandrus, D. G.; Xiao, D.; Yao, W.; et al. Electrical Control of Neutral and Charged Excitons in a Monolayer Semiconductor. *Nat. Commun.* **2013**, *4*, 1474.
11. Lu, X.; Utama, M. I.; Lin, J.; Gong, X.; Zhang, J.; Zhao, Y.; Pantelides, S. T.; Wang, J.; Dong, Z.; Liu, Z.; et al. Large-Area Synthesis of Monolayer and Few-Layer $MoSe_2$ Films on SiO_2 Substrates. *Nano Lett.* **2014**, *14*, 2419–2425.
12. Ye, Z.; Cao, T.; O'Brien, K.; Zhu, H.; Yin, X.; Wang, Y.; Louie, S. G.; Zhang, X. Probing Excitonic Dark States in Single-Layer Tungsten Disulphide. *Nature* **2014**, *513*, 214–218.
13. Zhu, B.; Zeng, H.; Dai, J.; Gong, Z.; Cui, X. Anomalously Robust Valley Polarization and Valley Coherence in Bilayer WS_2. *Proc. Natl. Acad. Sci. U.S.A.* **2014**, *111*, 11606–11611.
14. Jones, A. M.; Yu, H. Y.; Ghimire, N. J.; Wu, S. F.; Aivazian, G.; Ross, J. S.; Zhao, B.; Yan, J. Q.; Mandrus, D. G.; Xiao, D.; et al. Optical Generation of Excitonic Valley Coherence in Monolayer WSe_2. *Nat. Nanotechnol.* **2013**, *8*, 634–638.
15. Clark, G.; Wu, S. F.; Rivera, P.; Finney, J.; Nguyen, P.; Cobden, D. H.; Xu, X. D. Vapor-Transport Growth of High Optical Quality WSe_2 Monolayers. *APL Mater.* **2014**, *2*, 101101.
16. Wang, G.; Bouet, L.; Lagarde, D.; Vidal, M.; Balocchi, A.; Amand, T.; Marie, X.; Urbaszek, B. Valley Dynamics Probed through Charged and Neutral Exciton Emission in Monolayer WSe_2. *Phys. Rev. B* **2014**, *90*, 075413.
17. Zhang, Y. J.; Oka, T.; Suzuki, R.; Ye, J. T.; Iwasa, Y. Electrically Switchable Chiral Light-Emitting Transistor. *Science* **2014**, *344*, 725–728.
18. Thilagam, A. Exciton Complexes in Low Dimensional Transition Metal Dichalcogenides. *J. Appl. Phys.* **2014**, *116*, 053523.
19. Berkelbach, T. C.; Hybertsen, M. S.; Reichman, D. R. Theory of Neutral and Charged Excitons in Monolayer Transition Metal Dichalcogenides. *Phys. Rev. B* **2013**, *88*, 045318.
20. Hsu, W. T.; Zhao, Z. A.; Li, L. J.; Chen, C. H.; Chiu, M. H.; Chang, P. S.; Chou, Y. C.; Chang, W. H. Second Harmonic Generation from Artificially Stacked Transition Metal Dichalcogenide Twisted Bilayers. *ACS Nano* **2014**, *8*, 2951–2958.
21. Fang, H.; Battaglia, C.; Carraro, C.; Nemsak, S.; Ozdol, B.; Kang, J. S.; Bechtel, H. A.; Desai, S. B.; Kronast, F.; Unal, A. A.; et al. Strong Interlayer Coupling in van der Waals Heterostructures Built from Single-Layer Chalcogenides. *Proc. Natl. Acad. Sci. U.S.A.* **2014**, *111*, 6198–6202.
22. Chiu, M. H.; Li, M. Y.; Zhang, W.; Hsu, W. T.; Chang, W. H.; Terrones, M.; Terrones, H.; Li, L. J. Spectroscopic Signatures for Interlayer Coupling in MoS_2-WSe_2 van der Waals Stacking. *ACS Nano* **2014**, *8*, 9649–9656.
23. Roy, T.; Tosun, M.; Kang, J. S.; Sachid, A. B.; Desai, S. B.; Hettick, M.; Hu, C. C.; Javey, A. Field-Effect Transistors Built from All Two-Dimensional Material Components. *ACS Nano* **2014**, *8*, 6259–6264.
24. Furchi, M. M.; Pospischil, A.; Libisch, F.; Burgdorfer, J.; Mueller, T. Photovoltaic Effect in an Electrically Tunable van der Waals Heterojunction. *Nano Lett.* **2014**, *14*, 4785–4791.
25. Cheng, R.; Li, D.; Zhou, H.; Wang, C.; Yin, A.; Jiang, S.; Liu, Y.; Chen, Y.; Huang, Y.; Duan, X. Electroluminescence and Photocurrent Generation from Atomically Sharp WSe_2/MoS_2 Heterojunction P-N Diodes. *Nano Lett.* **2014**, *14*, 5590–5597.
26. Lee, C. H.; Lee, G. H.; van der Zande, A. M.; Chen, W.; Li, Y.; Han, M.; Cui, X.; Arefe, G.; Nuckolls, C.; Heinz, T. F.; et al. Atomically Thin P-N Junctions with van der Waals Heterointerfaces. *Nat. Nanotechnol.* **2014**, *9*, 676–681.
27. Gong, Y.; Lin, J.; Wang, X.; Shi, G.; Lei, S.; Lin, Z.; Zou, X.; Ye, G.; Vajtai, R.; Yakobson, B. I.; et al. Vertical and In-Plane Heterostructures from WS_2/MoS_2 Monolayers. *Nat. Mater.* **2014**, *13*, 1135–1142.
28. Murata, H.; Koma, A. Modulated STM Images of Ultrathin $MoSe_2$ Films Grown on MoS_2(0001) Studied by STM/STS. *Phys. Rev. B* **1999**, *59*, 10327–10334.
29. Zhang, X.; Meng, F.; Christianson, J. R.; Arroyo-Torres, C.; Lukowski, M. A.; Liang, D.; Schmidt, J. R.; Jin, S. Vertical Heterostructures of Layered Metal Chalcogenides by van der Waals Epitaxy. *Nano Lett.* **2014**, *14*, 3047–3054.
30. Tongay, S.; Fan, W.; Kang, J.; Park, J.; Koldemir, U.; Suh, J.; Narang, D. S.; Liu, K.; Ji, J.; Li, J.; et al. Tuning Interlayer Coupling in Large-Area Heterostructures with CVD-Grown MoS_2 and WS_2 Monolayers. *Nano Lett.* **2014**, *14*, 3185–3190.
31. Huo, N.; Kang, J.; Wei, Z.; Li, S.-S.; Li, J.; Wei, S.-H. Novel and Enhanced Optoelectronic Performances of Multilayer MoS_2-WS_2 Heterostructure Transistors. *Adv. Funct. Mater.* **2014**, *24*, 7025–7031.
32. Lam, K. T.; Seol, G.; Guo, J. Operating Principles of Vertical Transistors Based on Monolayer Two-Dimensional Semiconductor Heterojunctions. *Appl. Phys. Lett.* **2014**, *105*, 013112.
33. Li, M.; Esseni, D.; Snider, G.; Jena, D.; Xing, H. G. Single Particle Transport in Two-Dimensional Heterojunction Interlayer Tunneling Field Effect Transistor. *J. Appl. Phys.* **2014**, *115*, 074508.
34. Tonndorf, P.; Schmidt, R.; Bottger, P.; Zhang, X.; Borner, J.; Liebig, A.; Albrecht, M.; Kloc, C.; Gordan, O.; Zahn, D. R. T.; et al. Photoluminescence Emission and Raman Response of Monolayer MoS_2, $MoSe_2$, and WSe_2. *Opt. Express* **2013**, *21*, 4908.
35. Zhao, W. J.; Ghorannevis, Z.; Chu, L. Q.; Toh, M. L.; Kloc, C.; Tan, P. H.; Eda, G. Evolution of Electronic Structure in Atomically Thin Sheets of WS_2 and WSe_2. *ACS Nano* **2013**, *7*, 791–797.
36. Peimyoo, N.; Shang, J. Z.; Cong, C. X.; Shen, X. N.; Wu, X. Y.; Yeow, E. K. L.; Yu, T. Nonblinking, Intense Two-Dimensional Light Emitter: Mono Layer WS_2 Triangles. *ACS Nano* **2013**, *7*, 10985–10994.
37. Kang, J.; Tongay, S.; Zhou, J.; Li, J. B.; Wu, J. Q. Band Offsets and Heterostructures of Two-Dimensional Semiconductors. *Appl. Phys. Lett.* **2013**, *102*, 012111.
38. Gong, C.; Zhang, H. J.; Wang, W. H.; Colombo, L.; Wallace, R. M.; Cho, K. J. Band Alignment of Two-Dimensional Transition Metal Dichalcogenides: Application in Tunnel Field Effect Transistors. *Appl. Phys. Lett.* **2013**, *103*, 053513.
39. He, J. G.; Hummer, K.; Franchini, C. Stacking Effects on the Electronic and Optical Properties of Bilayer Transition Metal Dichalcogenides MoS_2, $MoSe_2$, WS_2, and WSe_2. *Phys. Rev. B* **2014**, *89*, 075409.

40. Lu, N.; Guo, H. Y.; Li, L.; Dai, J.; Wang, L.; Mei, W. N.; Wu, X. J.; Zeng, X. C. $MoS2_2/MX_2$ Heterobilayers: Bandgap Engineering *via* Tensile Strain or External Electrical Field. *Nanoscale* **2014**, *6*, 2879–2886.
41. Lu, N.; Guo, H.; Wang, L.; Wu, X.; Zeng, X. C. Van der Waals Trilayers and Superlattices: Modification of Electronic Structures of MoS_2 by Intercalation. *Nanoscale* **2014**, *6*, 4566–4571.
42. Schmidt, T.; Lischka, K.; Zulehner, W. Excitation-Power Dependence of the Near-Band-Edge Photoluminescence of Semiconductors. *Phys. Rev. B* **1992**, *45*, 8989–8994.
43. Vietmeyer, F.; Frantsuzov, P. A.; Janko, B.; Kuno, M. Carrier Recombination Dynamics in Individual CdSe Nanowires. *Phys. Rev. B* **2011**, *83*, 115319.
44. Reshchikov, M. A.; Olsen, A. J.; Bishop, M. F.; McMullen, T. Superlinear Increase of Photoluminescence with Excitation Intensity in Zn-doped GaN. *Phys. Rev. B* **2013**, *88*, 075204.
45. Hong, X.; Kim, J.; Shi, S. F.; Zhang, Y.; Jin, C.; Sun, Y.; Tongay, S.; Wu, J.; Zhang, Y.; Wang, F. Ultrafast Charge Transfer in Atomically Thin MoS_2/WS_2 Heterostructures. *Nat. Nanotechnol.* **2014**, *9*, 682–686.
46. Ceballos, F.; Bellus, M. Z.; Chiu, H. Y.; Zhao, H. Ultrafast Charge Separation and Indirect Exciton Formation in a MoS_2-$MoSe_2$ van der Waals Heterostructure. *ACS Nano* **2014**, *8*, 12717–12724.